International Journal of Pharmaceutics 632 (2023) 122574

Contents lists available at ScienceDirect

International Journal of Pharmaceutics

journal homepage: www.elsevier.com/locate/ijpharm

3D printing of LEGO® like designs with tailored release profiles for treatment of sleep disorder

Atabak Ghanizadeh Tabriz [a], Md Sadeque Mithu [c], Milan D. Antonijevic [b], Lilian Vilain [d], Youri Derrar [d], Clara Grau [e], Anaïs Morales [e], Orestis L. Katsamenis [f], Dennis Douroumis [a,b,*]

[a] Delta Pharmaceutics Ltd, 20 Steven Close, Chatham, Kent ME4 5NG, UK
[b] University of Greenwich, Faculty of Engineering and Science, School of Science, Chatham Maritime, Chatham, Kent ME4 4TB, UK
[c] Cubi-Tech Extrusion Ltd, 3 Sextant Park, Neptune Close, Rochester, Chatham, Kent ME2 4LU, UK
[d] Aix Marseille Université, Polytech Marseille, School of Engineering, 3 Avenue of Luminy, 13009 Marseille, France
[e] University of Haute-Alsace (UHA), School of Chemistry of Mulhouse (ENSCMu), 3 Street Alfred Werner, 68093 Mulhouse, France
[f] University of Southampton, μ-VIS X-ray Imaging Centre, Faculty of Engineering and Physical Sciences, Southampton SO17 1BJ, UK

ARTICLE INFO

Keywords:
3D printing
LEGO®-like designs
Compartmental systems
Personalised treatment

ABSTRACT

3D printed LEGO®-like designs are an attractive approach for the development of compartmental delivery systems due to their potential for dose personalisation through the customisation of drug release profiles. Additive manufacturing technologies such as Fused Deposition Modelling (FDM) are ideal for the printing of structures with complex geometries and various sizes. This study is a paradigm for the fabrication of 3D printed LEGO® -like tablets by altering the design of the modular units and the filament composition for the delivery of different drug substances. By using a combination of placebo and drug loaded compartments comprising of immediate release (hydroxypropyl cellulose) and pH dependant polymers (hypromellose acetate succinate) we were able to customise the release kinetics of melatonin and caffeine that can potentially be used for the treatment of sleep disorders. The LEGO® -like compartments were designed to achieve immediate release of melatonin followed by variable lag times and controlled release of caffeine.

1. Introduction

Three-dimensional (3D) printing has received increasing attention in various sectors such as aerospace, art, architecture, fashion, space and particularly in pharmaceutical and medical industry. The potential processibility of pharmaceutical grade polymers and several active ingredients (APIs) has transformed 3D printing into an emerging technology that can be employed for customised designs and personalised treatment for improved patient life quality (Sandler and Preis, 2016; Araújo et al., 2019). A wide range of 3D printing technologies have been introduced for the development of personalised dosage forms such as selective laser sintering (SLS) (Kulinowski et al., 2021), Fused deposition modelling (FDM) (Scoutaris et al., 2018; Tabriz et al., 2021); Stereolithography (SLA) (Goyanes et al., 2016; Wang et al., 2016), inkjet printing (Chao et al., 2021; Lion et al., 2021) and semi-solid/paste extrusion (Tagami et al., 2021; Khaled et al., 2018). 3D printing offers several advantages over conventional processes such as the fabrication of complex tablet geometries, incorporation of several APIs (polypills) (Lion et al., 2021; Xu et al., 2020) and the tailoring of the API release according to the desired specifications (Martinez et al., 2018; Ghanizadeh Tabriz et al., 2020).

Several studies have investigated the capability of FDM printing on dual release profiles for specific disease treatment (Araújo et al., 2019; Cunha-Filho et al., 2017; Pinho et al., 2021). Ghanizadeh Tabriz et al. (2020) developed a 3D printed bilayer tablet for the co-delivery of isoniazid (INZ) and rifampicin (RFC) to treat tuberculosis. By using a combination of hydrophilic and pH dependent polymers it was possible to meet INZ release in acidic media while RFC in pH $>$ 5.5 from open design tablets. Sadia et al. (2018) employed a dual FDM printer to print bilayer tablets for potential treatment of hypertension. The printed designs featured two compartments, loaded with hydrochlorothiazide and enalapril maleate. Several designs with various doses were printed to evaluate the potential of FDM technology for personalised medication. Depending on the design and the API loading different release profile patterns for APIs were observed within 60 min in pH 1.2.

An interesting approach has been recently introduced for the

* Corresponding author.
E-mail address: d.douroumis@gre.ac.uk (D. Douroumis).

https://doi.org/10.1016/j.ijpharm.2022.122574
Received 8 October 2022; Received in revised form 28 December 2022; Accepted 29 December 2022
Available online 2 January 2023

development of drug multimodal release profiles using LEGO® – inspired devices for personalised dosage forms (Tan et al., 2020). Based on such designs, modular units are fabricated based on different geometries, polymer composition, loading of various drugs or placebo compartments which enable customized oral dosage forms. The combined advantages of FDM and LEGO® -like designs allows to use swellable, eroding hydrophilic or pH dependent polymers which provides an unlimited capacity of customized products. Rycerz et al., reported the development of LEGO® -like chewable brick for the delivery of paracetamol and ibuprofen as model APIs by extruding semi-solid formulations (Rycerz et al., 2019). Gelatin was used as the main drug carrier for the printing of specifically designed patterns and the fabrication of various doses. Melocchi et al., optimised LEGO® -inspired capsular devices that allow multimodal release of caffeine for personalised dietary supplements (Melocchi et al., 2020). By using FDM the capsular devices comprised of modular units of different polymers such as hydroxypropyl cellulose, polyvinyl alcohol, and (hydroxypropyl methylcellulose acetate succinate. The printed capsules were compared to those obtained by injection moulding to prove the rapid prototyping ability of 3D printing technology.

Sleep disorder (insomnia) has considerably been affecting 10–30 % of the world's population which potentially causes disruption of people's day to day activities (Bhaskar et al., 2016). Melatonin (MLT) is a hormone produced by pineal gland which is associated with sleep regulation. Melatonin tablets at various doses are usually prescribed to regulate sleep pattern for patients with sleep disorders. However, the use of MLT is associated with several side effects such as headache, short-term feelings of depression, daytime sleepiness and dizziness (Arendt, 1997).

The aim of this study is to co-administrate caffeine (CAF) with MLT. Primary MLT release ensures that the patient will fall sleep where a delayed release of caffeine can regulate the sleep time while avoiding or minimising the appearance of MLT's side effect. In this study, FDM printing is used to print LEGO® -like compartments of MLT and caffeine loaded filaments along with pH dependent placebo compartments. The compartments subsequently are assembled together into a round-shape tablet to ensure immediate release of MLT and delayed release of the caffeine. By altering the composition of CAF filaments either using hydrophilic or pH dependent polymers was feasible to control the release rates at desirable time points.

2. Materials and methods

2.1. Materials

Caffeine (CAF) and Polyethylene glycol (PEG) 6000 were purchased from Sigma-Aldrich (Gillingham, UK). Melatonin (MLT) was purchased from Tokyo Chemicals (Zwijndrecht, Belgium). Hydroxypropyl Cellulose (Klucel ELF) and Hypromellose acetate succinate (HMPCAS, AQOAT AS-LMP) were kindly donated by Ashland (Rotterdam, Netherlands) and Shin–Etsu (Tokyo, Japan) respectively.

2.2. Hot melt extrusion for fabrication of 3D printing filaments

Four physical blends were prepared for hot melt extrusion of drug loaded and placebo 3D printing filaments. First blend comprised of Klucel ELF/MLT at 90/10 (wt/wt). The second blend comprised of Klucel ELF/caffeine at 70/30 (wt/wt). The third blend comprised of AS-LMP/PEG/caffeine at 60/10/30 (wt/wt). The placebo blend comprised of AS-LMP/PEG 6000 at 85/15 (wt/wt).

The drug/polymer formulations were blended in a turbula shaker-mixer (Glen Mills T2F Shaker/Mixer, Clifton, UK) at 75 rpm for 10 min to ensure the blends are fully homogenous. All four blends were extruded using a 16 mm twin-screw extruder (Eurolab 16, Thermo Fisher, Germany). The extruder feed rate was set to 10 g/min. Extrusion settings for all drug loaded and placebo filaments are shown in Table 1. The filament diameter was accurately controlled using a 3D line (Rondol Industries, France). The filament was fed through a laser diameter measuring gauge connected to the hall-of-unit for precise control of the filament thickness due to the adjustable motor speed. Subsequently, the filament was loaded in the wind-up unit for collection on the appropriate spool. The filament thickness across the whole process was approximately 2.85 mm.

2.3. Design and 3D printing of Melatonin/caffeine/placebo compartments

The compartments of the tablets were designed via Solid Works V20 software (Dassault Systems, USA). The designs of the tablet compartments were initially converted from SolidWorks.prt files to stl files, a readable format for Cura slicing software (Ultimaker, Netherland) where printing files (Gcodes) were generated for the 3D printer. The 3D printing settings for each extruded filament and hence each compartment of the printed tablets is shown in Table 2. The MLT compartment is designed to release 6 mg in gastric pH by co-processing of ELF/MLT blends. The CAF compartment is designed in a manner to carry approximately 50 mg of caffeine. Two sized placebo compartments were designed with various thicknesses to ensure caffeine's release lag times. The total size of the tablet was set at 13 mm diameter and a 5 mm height. All four filaments were printed using an Ultimaker 3 extended (Ultimaker, Netherlands). The AA0.4 print core (Nozzle diameter: 0.4 mm) was used for the fabrication of all tablet compartments.

2.4. Thermal gravimetric analysis (TGA)

Thermal stability of the bulk materials and the extruded filaments were examined via TGA (TGA, TA instruments, USA). 2–2.5 mg of each respective sample was weighed and loaded into a standard TGA aluminium pan. The samples were heated from 25 °C to 500 °C at a rate of 10 °C/min under 50 mL/min Nitrogen purge in the balance chamber. The generated data was analysed via TA Universal Analysis software (Universal Analysis version 2000, USA).

2.5. Differential scanning calorimetry (DSC)

A differential scanning calorimeter (Mettler-Toledo 823e,

Table 1
Extrusion settings and processing paraments for fabrication of drug loaded and placebo filaments.

Formulation	Composition (ratio)	Zone 1 (°C)	Zone 2 (°C)	Zone 3 (°C)	Zone 4 (°C)	Zone 5 (°C)	Zone 6 (°C)	Zone 7 (°C)	Zone 8 (°C)	Zone 9 (°C)	Die (°C)
F1	ELF/MLT (90/10)	35	55	85	130	150	150	150	150	150	130
F2	ELF/CAF (70/30)	35	55	85	130	150	150	150	150	150	130
F3	AS-LMP/PEG/CAF (60/10/30)	40	55	75	100	140	140	140	140	140	120
F4	AS-LMP/PEG (85/15)	40	55	75	100	160	160	160	160	160	140

Greifensee, Switzerland) was used to assess DSC thermograms of the bulk materials. samples (2–2.5 mg) were placed into a 40 μL aluminium pan and crimped promptly. The temperature range set for the method varied for each sample. The samples were heated at a 10 °C/min heating rate. STARe Excellence Thermal Analysis Software was used to analyse the obtained DSc thermograms.

2.6. Scanning electron microscopy (SEM)

To assess the extruded filament's morphology and layer consistency of the 3D printed compartments for each formulation, scanning electron microscopy (Hitachi SU8030, Japan) was utilised. The SEM images of the filaments and the 3D printed tablet compartments were captured by an electron beam accelerating voltage of 2 kV and a magnification of 30 and 50X respectively.

2.7. X-ray powder diffraction (XRPD)

XPRD was used to investigate the physical state of the bulk materials as well the physical state of the MLT and caffeine in the extruded filaments. Samples from bulk materials and 3D printing filaments were placed between 2 sheets of Mylar for support and analysed in transmission mode. A D8 Advance diffractometer (Bruker, Germany) was used with Cu Kα radiation (40 kV, 40 mA) and a LynxEye silicon strip detector. A step size of 0.02° with a counting time of 0.3 s per step was used to collect data from 5 to 60° 2θ.

2.8. In vitro dissolution studies and high-performance liquid chromatography (HPLC) analysis

In-vitro drug release of MLT and CAF were studied using 900 mL of pH 1.2 and pH 4.5, 5.5 and 7.4 buffer, respectively. A Varian 705-DS (USA) dissolution bath equipped with a paddle apparatus were used for the study at 37 ± 0.5 ℃ and paddle rotation speed of 100 rpm. The tablets added into the 0.1 N hydrochloric acid media (pH 1.2) for 2 hr to simulate MLT release in the gastric environment. The pH of the media then was increased to 4.5 for an hour with addition of sodium hydroxide into the media to mimic the CAF release. The pH then was increased to 5.5 for another hour and subsequently, was adjusted to 7.4 for further four hours. For the purposes of the studies, 2 mL samples were withdrawn at 15, 30, 45, 60 min and then at 30 min time intervals for further 9 h. All samples were filtered and placed into an autosampler vials for HPLC analysis.

The release of MLT and CAF was determined using an Agilent technology 1200 series HPLC system (USA), equipped with a Agilent Zorbax Eclipse XDB-C18 (5 X 150 X 4.5 μm) column. An isocratic mobile phase consisted of Acetonitrile: water (60:40) were used at 1 mL/min flow rate with a stop time of 4.5 min per analysis. Both drug molecules were analysed at 275 nm using a UV detector. All the withdrawn sample solutions from the dissolutions were filtered using a 0.45 μm disk filter before analysis and studies were performed in triplicates.

2.9. Volumetric Imaging and characterisation by means of microfocus computed tomography (μCT).

X-ray microfocus computed tomography (μCT) was used to characterise the microstructure of the individual compartments of the solid dosage form in terms of overall volume, porosity, local thickness and visualise defects and imperfections. Each component was imaged separately to allow for accurate segmentation.

μCT imaging was performed using a customised μCT scanner optimised for 3D X-ray histology (https://www.xrayhistology.org) based on a Nikon's XTH225ST system (Nikon Metrology UK ltd) at the Biomedical Imaging Unit at University Hospital Southampton. Imaging was conducted at 100 kVp / 69 μA without any beam pre-filtration. The source to detector and source to object distances were 897.7 mm and 41.9 mm respectively, resulting in a voxel size of 14 μm. The 2850 × 2850 dexels detector was binned 2x resulting in a virtual detector of 1425 × 1425 dexels. Imaging parameters were as follows: 1901 projections were collected over the 360° rotation, with 8 frames per projection being averaged for each projection to improve the signal to noise ratio.

Reconstruction of the volume data, image processing and analysis: Following completion of each acquisition, data were automatically reconstructed into 32-bit volumes by means of Nikon's own reconstruction engine which uses a filtered-back projection algorithm. Each dataset was then resliced (re-oriented in space) and cropped in using Fiji / ImageJ (Schindelin et al., 2015) and the volumes were saved in 16-bit files. Porosity analysis, thickness analysis and visualisation were conducted in "Dragonfly" (v. 2021.3.0.1087; Object Research Systems (ORS) Inc, Montreal, Canada, 2020; software available at https://www.theobjects.com/dragonfly). The pores (internal defects), open space (designed macro-porosity) and the compartment's material were segmented using thresholding and manual refinement. The porosity analysis was conducted using the connected components tool applied on the segmented pores volume, and local thickness analysis using the "Volume Thickness Map" tool on the segmented object (material excluding pores). Local thickness is defined on a per voxel (3D pixel) basis as "the diameter of the largest sphere that fits inside the object and contains the voxel". Local thickness histograms visualise the number of voxels associated with a certain sphere diameter.

3. Results and discussions

3.1. Extrusion processing

MLT and CAF loaded filaments were extruded by coupling a 16 mm extruder with the 3D line in order to develop highly uniform and consistent filaments. It is important to fabricate filaments that feature minimal diameter tolerances (< ±10 %) that could be caused by over and/or under extrusion during the 3D printing process increasing the chances of printing failure. For the extrusion optimisation three different temperature profiles were applied while feed rate and screw speeds were kept constant to achieve suitable diameters. Feeding rates varied from 5

Table 2
FDM printing settings of the filaments.

Formulation	Composition (ratio)	Print speed (mm/s)	Printing temperature (°C)	Build plate temperature (°C)
F1	ELF/MLT (90/10)	10.0	170	80
F2	ELF/CAF (70/30)	5.0	150	40
F3	AS-LMP/PEG/CAF (60/10/30)	10.0	150	50
F4	AS-LMP/PEG (85/15)	10.0	160	60

to 10 g/h with the latter showing less thickness variability. The selection of the polymer carriers was based on their drug release capability (immediate or controlled) and printability. Both polymers have been studies in previous work (Tabriz et al., 2021) whereby the extruded filaments demonstrated appropriate tensile strength and hence good printability.

For this study the amorphicity of the APIs was not a crucial factor as MLT and CAF are freely soluble in water, therefore the goal of HME was to ensure to fabricate filaments with appropriate API content uniformity.

3.2. Thermal and solid-state analysis

Thermal stability of the bulk materials was investigated in order to identify the temperature threshold for extrusion optimisation and the manufacturing of the filaments. As shown in Fig. 1a the AS-LMP and Klucel ELF presented an initial 2 % mass loss due to moisture content and stability up to 200 °C and 250 °C respectively followed by gradual mass loss due to polymer degradation. Similarly, Caffeine, PEG 6000 and MLT showed thermal stability at 180 °C, 200 °C and 240 °C respectively where all exhibited a rapid mass loss due to degradation. As shown in Table 1, the findings of TGA analysis were used to optimise the extrusion temperature profiles for the placebo and drug loaded filaments.

Similarly, thermogravimetric analysis of extruded filaments was conducted to determine the appropriate printing temperature via FDM technology. As shown in Fig. 1b similar thermogravimetric profiles were obtained for the investigated filaments which were used for printing optimisation of the designed tablet components. Hence, as shown in Table 2 the printing temperatures varied from 150 to 170 °C in order to avoid any drug degradation during the 3D printing process.

DSC thermograms of the bulk materials used for fabrication of 3D printing filaments are shown in Fig. 2. PEG 6000 presented a sharp melting endotherm at 59.78 ℃ while MLT and caffeine at 118.30 ℃ and 234.34 ℃ respectively. In addition caffeine exhibited a weak endothermic peak which reflects to phase transition of caffeine from crystal form α to form β (Dong et al., 2007).Furthermore, Klucel ELF and AS-LMP showed glass transition (Tg) temperatures at 134.51 °C and 120.00 °C respectively.

X-ray diffraction was utilised to evaluate the physical state of bulk materials and the 3D printing filaments. As shown in Fig. 3a Klucel ELF and HMPCAS AS-LMP present two haloes with no visible peaks indicating their amorphous state. On the other hand, PEG 6000 exhibited two main peaks at 19.0° and 24.0° 2-theta. The MLT and caffeine crystalline state was confirmed through the presence of high intensity peaks at 11.7°, 26.2°, 27.1° 2 and at 16.2°, 24.2°, 25°, 26.1° 2-theta values respectively. However, as shown in Fig. 3b MLT turned

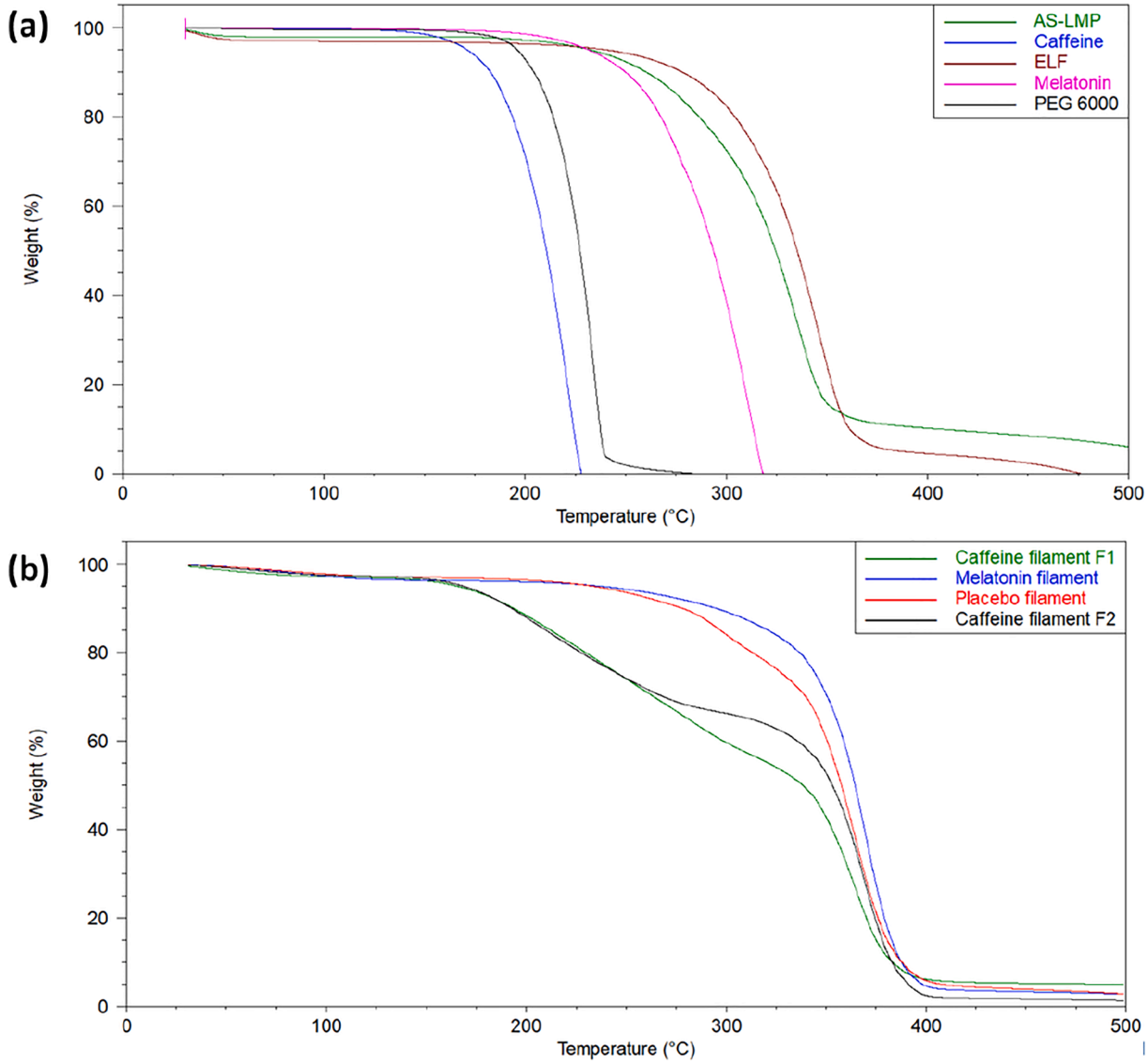

Fig. 1. TGA thermograms of (a) bulk materials and (2) the 3D printing filaments.

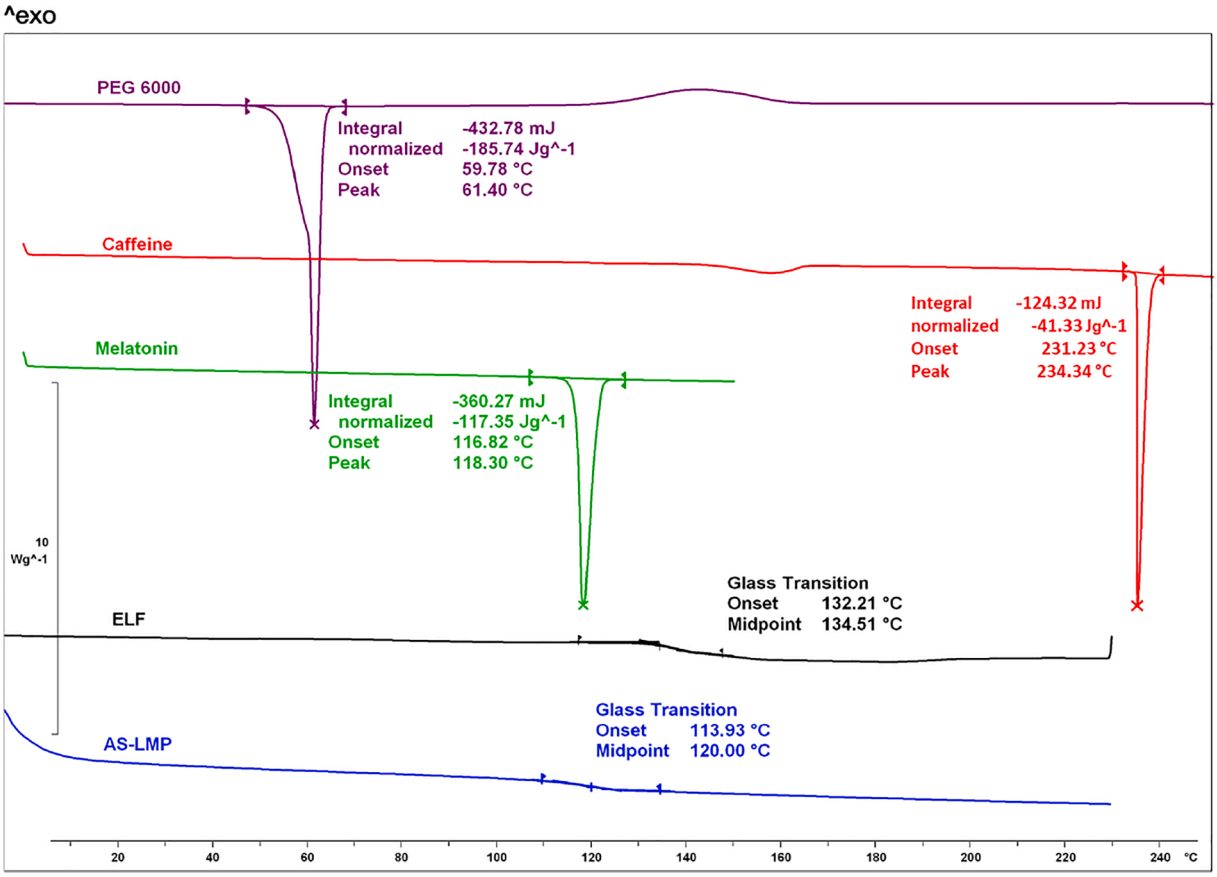

Fig. 2. DSC thermograms of bulk materials.

completely into amorphous state when co-extruded with the hydrophilic Klucel ELF. Similarly, the placebo filaments exhibit no peaks indicating the PEG 6000 has turned amorphous within the filament.

On the other hand, both caffeine loaded filaments present sharp peaks at 11.7° and 26.4 2-theta values indicating that the drug remained partially crystalline. Interestingly The second relative peak intensities of caffeine in the both filaments do not match that of the pure caffeine having particularly high intensities. This is indicative of significant preferred orientation of the caffeine within the filament (Christian et al., 2016). However, the remained crystalline fraction was not anticipated to affect the subsequent dissolution rates as caffeine is highly water-soluble.

3.3. 3D printing and assembly of the LEGO® like solid dosage forms

In this study the primary objective was to tailor the release the APIs by varying the polymer composition of the extruded filaments by taking in advantage the versatility of FDM technology which allows the processing of several thermoplastic polymers. Another objective was the design and the assembly of LEGO® -like compartments by tuning the formulation composition and the thickness of the placebo compartments. By adjusting the filament composition, the compartments can facilitate the required release profiles either by polymer dissolution at specific pH or erosion of the printed compartments. More specifically, ELF/MLT were co-extruded aiming to achieve rapid drug release in acidic pH 1.2 while CAF was processed with either ELF or AQOAT for controlled release at various rates. Furthermore, for the customization of the CAF release, the placebo LEGO® compartments comprised of the pH dependent polymer (HMPCAS-ASLMP) that dissolves at pH > 5.5.

As shown in Fig. 4 the tablet consists of four compartments that vary in thickness and filament composition. a) The tablet base consisted of a plain HPMCAS bucket shaped compartment featuring four indentations, b) the second compartment was composed of either an ELF/CAF or HPMCAS/CAF round shaped tablet for the release of the second API, c) a third plain HPMCAS compartment with variable thickness was used a seal closure (interlock with the HPMCAS base) to prevent any premature CAF release and d) a final donut shaped compartment was fitted on the overhang of the third compartment.

In Fig. 4 the first LEGO® -like design comprised of the placebo base compartment which had top, bottom and wall thickness of 0.4 mm. For the printing of the CAF compartment the ELF/CAF filament was used. The second design was identical to the first one and only the dimensions of the placebo base compartment were altered with 0.7 mm wall, 0.4 mm top and 0.4 mm bottom thickness respectively.

For the third LEGO® design the dimensions of the placebo base compartment were further increased with top, bottom and wall thickness of 1.2 mm while the CAF compartment comprised of HPMCAS/CAF formulation. The MLT compartments for all three designs were identical with 0.8 mm thickness and 13 mm diameter. The placebo and MLT compartments were printed at 100 % and 40 % infill density while the

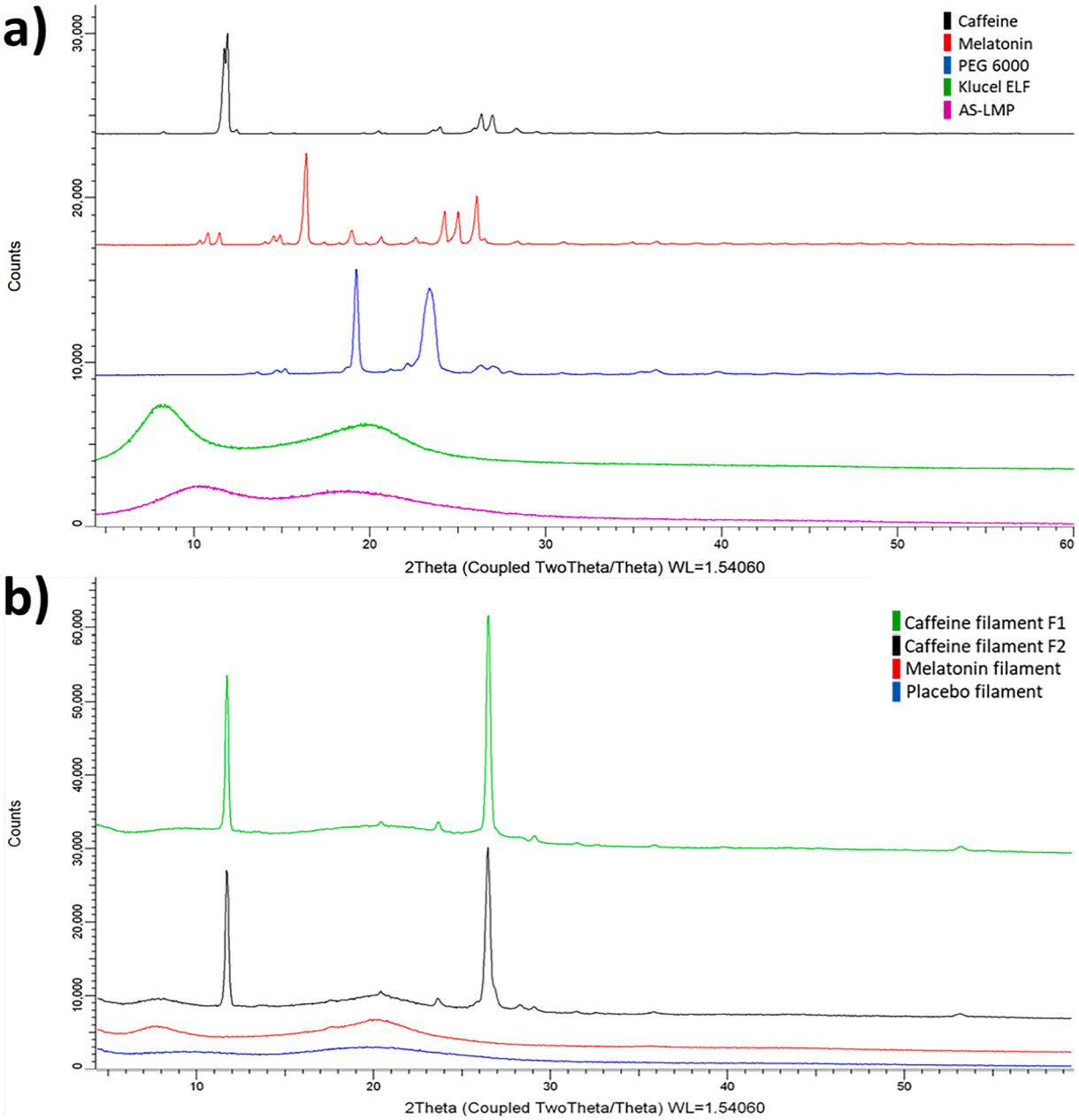

Fig. 3. XRD graphs of (a) plain materials and 3D printing drug loaded and placebo filaments.

CAF compartments at 60 % regardless of the respective formulations (F2, F3).

As shown in Fig. 5a the assembling of the four compartments formed a single round shaped tablet (13 × 5 mm) with unique features. It is obvious that the particular LEGO® design can be used for the delivery of a variety of drug substances while the total amount can be easily adjusted by either increasing the compartment thickness or the tablet diameter. Another advantage is that both compartments comprising of plain HPMCAS could be replaced by other eroding (e.g., HPMC) or swellable (Metolose, Polyox) polymers to achieve specific release profiles. The main purpose of using such polymer is to control and tune the lag times.

The 3D printing line facilitated the extrusion and collection of filaments with consistent target diameter and no fluctuations through the continuous monitoring with the laser diameter measuring gauge (Ponsar et al., 2020) As a result, minimum printing variability was observed from the nominal values of the CAD designed compartments combined with layer reproducibility and excellent surface finishing (see SEM analysis). Furthermore, weight reproducibility of printed compartments with different geometries was satisfactory (<5%) and met Ph.Eur. 2.9.5 guidelines.

SEM was used to further analyse the surface of the extruded filaments as well as the surface and consistency of the 3D printed compartments. As shown in Fig. 6 the MLT loaded and placebo filaments feature very smooth surfaces indicating that the extrusion processing parameters were fully optimised. On the other hand, CAF loaded filaments, presented consistent diameter throughout the filament, but with rough morphology which visible on the SEM scanned surfaces. This is attributed to the high API loading within the extruded blend. Similar filament morphologies have been observed by Krause et al even at lower CAF loadings (Krause et al., 2021).

In order to assess print quality for each extruded filament, tablet

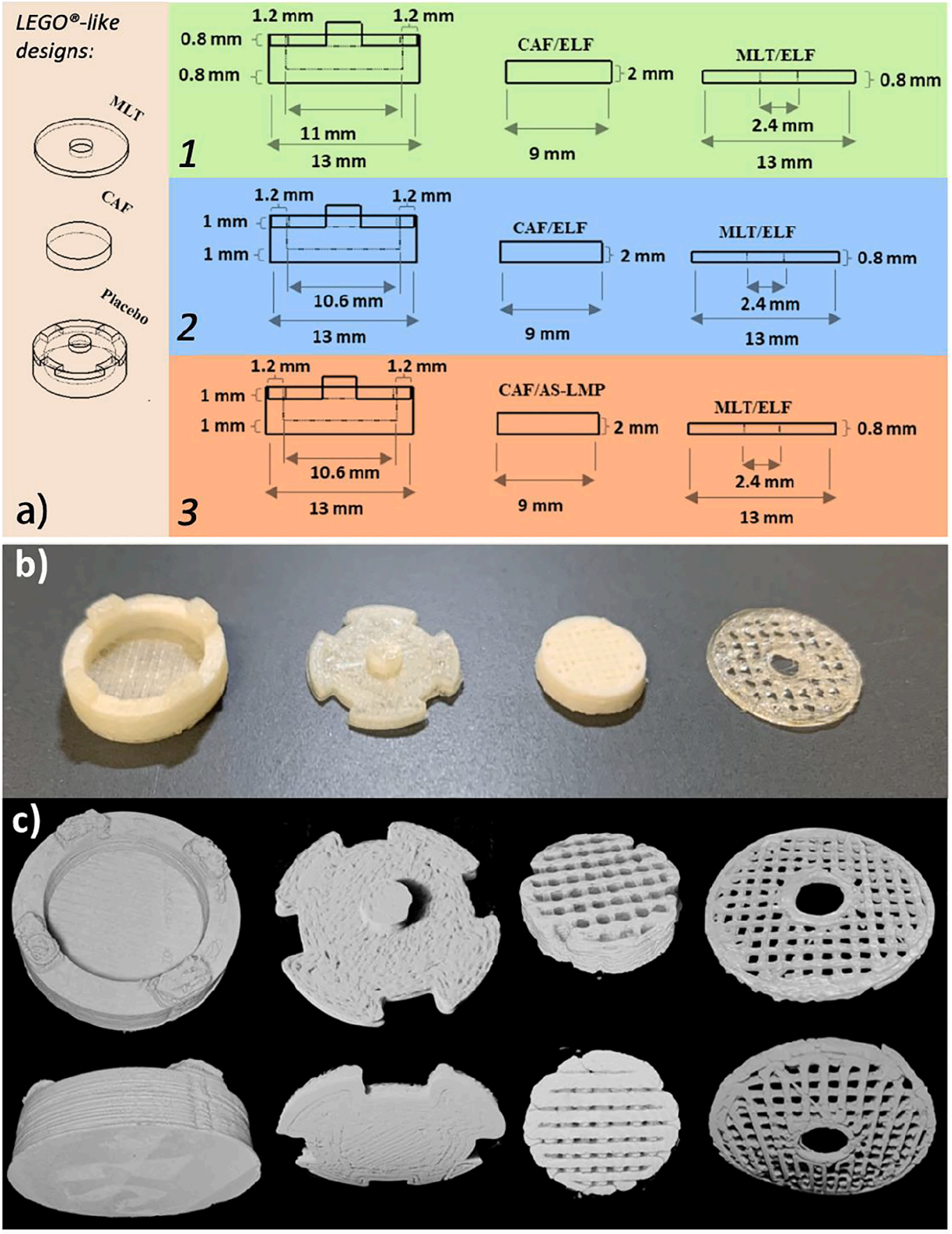

Fig. 4. (a) Design, (b) 3D printed and (c) X-ray CT rendering of the 3D printed compartments of the solid dosage form. From left to right; bottom compartment of the placebo section, top compartment of the placebo section, caffeine compartment and MLT compartment.

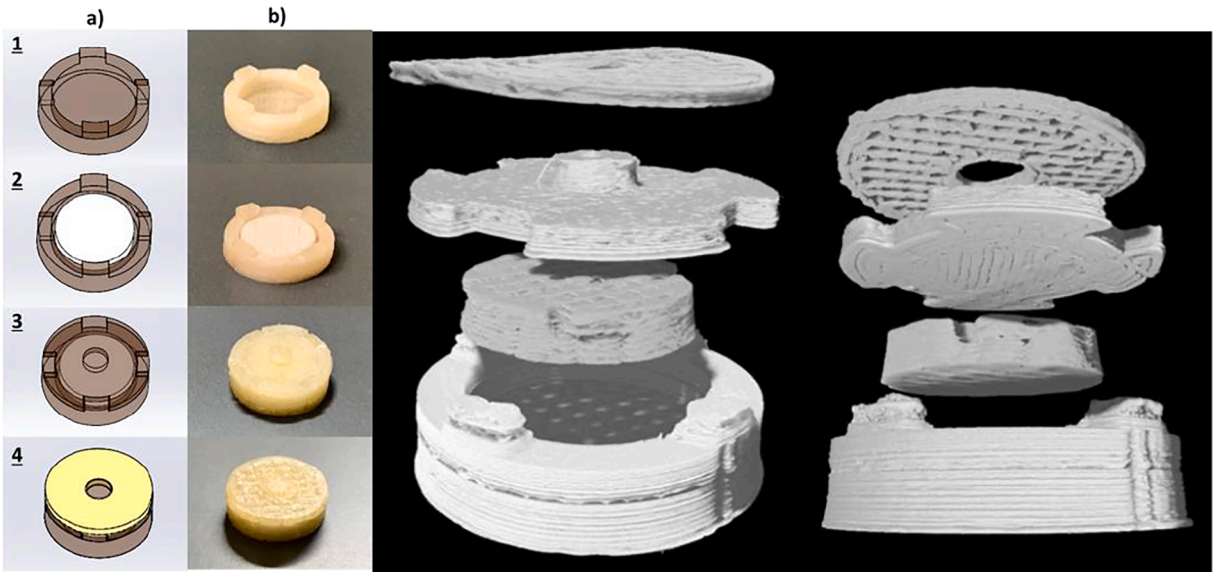

Fig. 5. Step by step assembly process of the LEGO® like solid dosage forms in (a) CAD and (b) 3D printed format, (c) in silico assembly of the individual compartment in the X-ray CT space.

designs with 12 mm diameter and 4 mm height were printed using the print settings shown in Table 2. The consistency of 3D printed layers is highly desirable in FDM technology and is directly correlated with optimum printing setting and consistent filament thickness (Ponsar et al., 2020). As shown in Fig. 6 all four printed formulations exhibit excellent printability with high consistency and reproducible layer thickness.

The average layer thickness of placebo and MLT filaments were 103.7 ± 11.6 and 104.5 ± 6.8 while for the F2 and F3 at 103.6 ± 7.51 and 105.03 ± 13.16 respectively.

3.4. Drug release studies

An important aspect for the design and printing of LEGO® -like modular devise is to achieve excellent quality where the designed gaps match perfectly those obtained after printing and consequently tightly sealed tablets are assembled. The sealing of the compartments is particularly important for the CAF. As shown in Fig. 7 the release profiles of MLT and CAF was investigated in a range of media varying from acidic (pH 1.2) to alkaline (pH 7.4). The ELF/MLT compartment for all LEGO® designs presented rapid dissolution rates with>80 % been detected in 30 min. The ELF is a non-ionic water-soluble thermoplastic polymer which is known for its printability (Tabriz et al., 2021).

As mentioned above the CAF release was controlled by the thickness of the placebo HPMCAS compartments and the formulations compositions. From Fig. 7 it is evident that the compartments were tightly sealed as no premature release of CAF was noticed for at least 4.5 h. In addition, HPMCAS showed very good resistance in acidic media and dimensional stability as well. For the LEGO® like design-1 CAF was released immediately after the pH change at 7.4 due to the thin wall thickness of the HPMCAS base unit and the rapid dissolution of the ELF/CAF compartment (>80 % within 30 min). The similar LEGO® -like design 2 showed slower release rate as a result of the thicker dimensions of the base unit. The slower CAF rate was attributed to the increased wall thickness (0.7 mm) which allowed directional release from the top part of the assembly.

A longer lag time was observed for the LEGO® -like design 3 where no CAF was observed for almost 5 h followed by sustained release for another 5 h until it was completely released (100 %). As expected, the thicker dimensions (1.2 mm) of the base unit led to even slower CAF release. The concept of altering the wall thickness of the various compartments and the formulations composition is not unknown and has been well studied by another group (Melocchi et al., 2020; Maroni et al., 2017) in capsular systems. Our findings are similar to those previously reported which however encounter inconsistencies due to the material selection (e.g., gelatine) and filament quality for the 3D printed modular parts (moulded parts showed better performance). Nevertheless, our study demonstrated that the optimisation of filament fabrication and print settings is a prerequisite to achieve reproducible and consistent control on the drug release rates.

3.5. Volumetric characterisation by means of μCT

For the purposes of this study μCT was used as a non-destructive imaging technique to investigate the 3D printed modular tablets. More specifically, μCT was employed to analyse the structure of the various tablet compartments and provide information about their integrity, layer structure and porosity. The latter is an important characteristic that was used to relate drug dissolution rates but also possible fabrication defects.

As previously mentioned, the placebo compartment units were designed at 100 % infill density to control the CAF release rates and prevent inflow of dissolution media. The μ-CT analysis (Fig. 8a-b) showed no open space porosity for closed volume. However, as shown in Fig. 8a and in Supplemental Video 1 an unexpected micro-porosity of 20.2 % was observed for the top placebo compartment consisting of a major interconnected pores network (Fig. 8a; top left) and a population of individual micro-pores. The porosity can be attributed to the print pattern of the slicing software, printing rate and temperature which result in incomplete fusion, and/or filament defects, all of which can lead to printing defects.

To the contrary the bottom placebo compartment showed an overall 0.3 % porosity which is in very good agreement with the desired print specifications. This was also evidenced from the obtained dissolution profiles which allowed control of CAF release only from the top placebo compartment while the bottom one was tightly packed and provided a waterproof environment for the CAF unit. As it can be seen in Fig. 9b and in Supplemental Video 2 the majority of the defect pores appear in the top-half of the compartment and develop as concentring / non-connected arc-shaped microchannels, without any detrimental effect on the overall integrity or permeability. As before this imperfection is

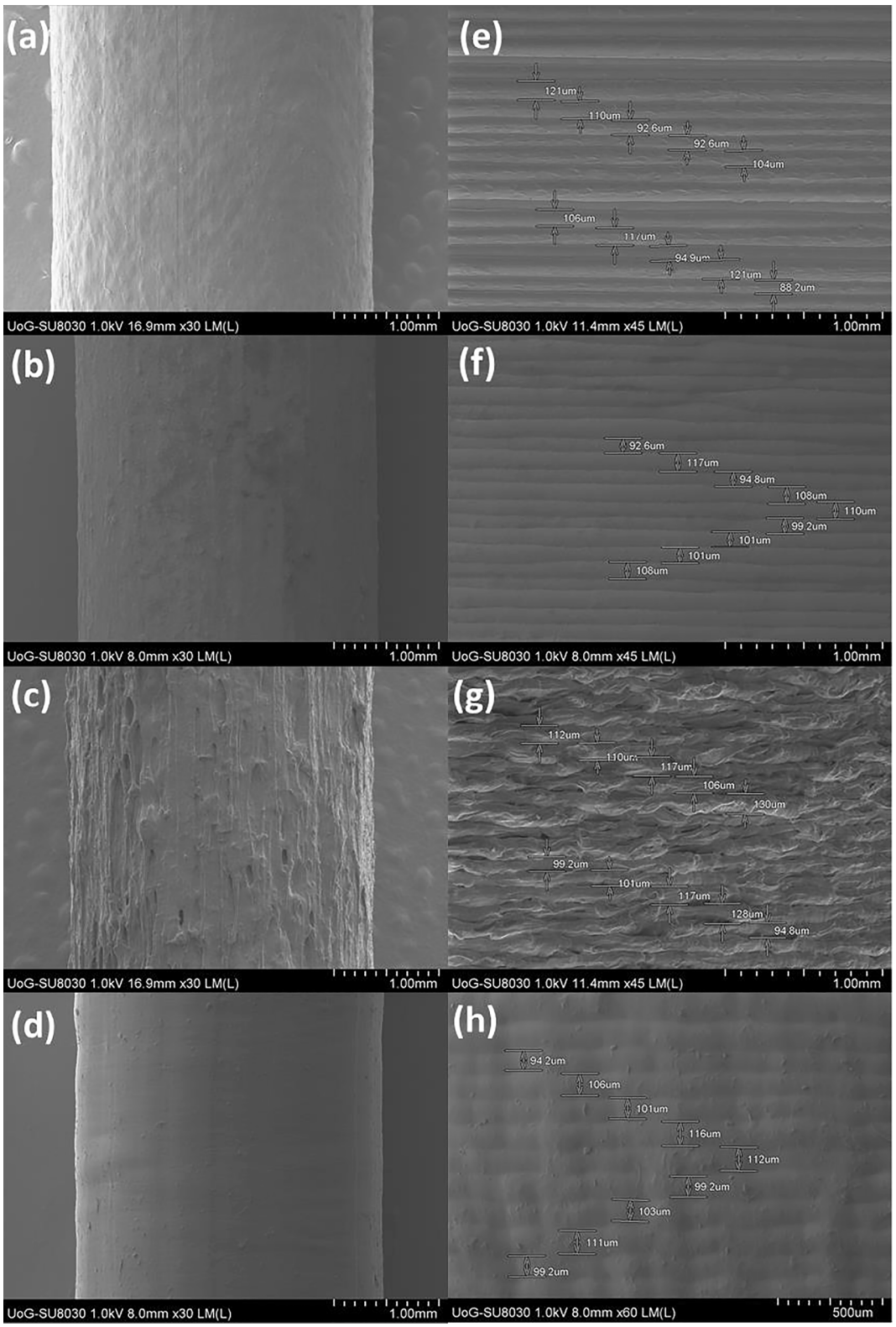

Fig. 6. SEM images of hot melt extruded (a) placebo, (b) AS-LMP/PEG/CAF, (c) CAF/ELF, and (d) MLT 3D printing filaments. SEM images of 3D printed (e) placebo, (d) AS-LMP/PEG/CAF, (c) CAF/ELF, and (d) MLT tablets.

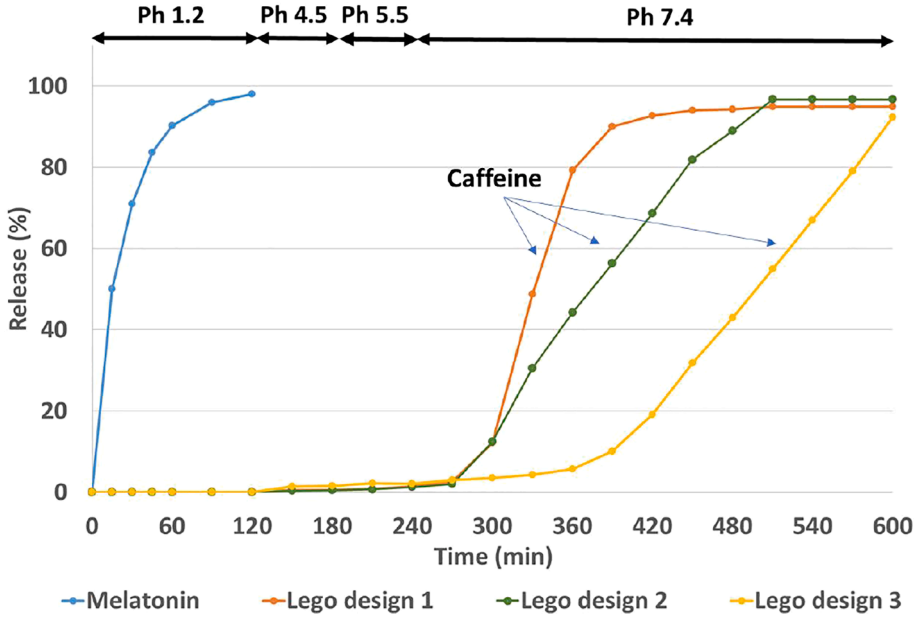

Fig. 7. l MLT release for all Lego designs and caffeine release evaluation from Lego design1,2 and 3.

related to the printing pattern of the software and it should be taken into account in future studies when a waterproof compartment is designed. We strongly believe that this significant difference in defect porosity between the two placebo compartments can be attributed to the nozzle printing path. In the former case (top placebo compartment) the nozzle followed a circular printing path deploying a coordinated motion of the X and Y actuators while the latter (bottom placebo compartment) was printed using a mixture of "parallel strokes" for the bottom part of the compartment and a circular printing path for the top-part, where the defect pores made their appearance. Circular printing seems to be much less "sensitive" to actuators errors (mechanical backlash, thermal drift, vibrations, etc). As a result, lay of material was more consistent allowing for better fusion and fewer defect pores (Farzadi et al., 2014).

Fig. 9 and Supplemental Video 3 illustrates μCT images of the MLT printed unit with an open space of 41.9 % which is in a good agreement with the designed infill density of 60 % (deviation of c. 2 %), while the determined defect micro-porosity was found to be 0.2 % over the closed volume, which excluded the "core" of the compartment. In Fig. 9d Supplemental Video 4 the analysed CAF compartment showed 33.2 % open space porosity against the 40 % of the designed porosity and 2.2 % defect micro-porosity for the printed design.

The findings for the MLT and CAF micro-porosity values are directly related to the quality of the extruded filaments as observed by SEM analysis. The filaments with smooth surface morphology (e.g., MLT) present better printability with less defects during printing and thus very low micro-porosity values while filaments with uneven surface (e.g., CAF) result in inconsistent printing and pore defects. Overall, μCT analysis played a critical role in determining the print quality of the printed modular units and identify any discrepancies with the designed structures. The technique is an excellent tool for further dosage optimisation and evaluation of the printing process.

μCT analysis also allowed accurate quantification of global measures such as the maximum feret diameter of the printed compartments, which can be interpreted as the largest linear distance between two opposing surface points akin to a calliper measure. The maximum feret diameter of a cuboidal shape for example, would return the maximum diagonal distance. The CAF compartment for example was designed with 9.0 mm diameter and 2.0 mm thickness (Fig. 4a), which results in a theoretical maximum calliper distance of 9.22 mm ($=\sqrt{9^2+2^2}$).

Our analysis returned the following maximum Feret diameter values for the four compartments: MLT: 13.48 mm; CAF: 9.33 mm; Top placebo: 13.35 mm; Bottom placebo: 14.06 mm, expressing variation from the theoretical values in the order of $+1.2\%_{(CAF)}$, $+3.5\%_{(MLT)}$, $+2.5\%_{(TopPlacebo)}$, $+1.1\%_{(BotomPlacebo)}$.

That is a variation < 5 % across all compartments, which shows a good agreement with the nominal values. It is also worth noting that the use of μCT as a measuring tool allows assessment of the whole volume and reducing the bias introduced by manual measurements.

4. Conclusions

In this study a LEGO® -like approach was implemented for the design of compartmental oral drug delivery systems comprising of assembled modular units. By using FDM printing technology, it was possible to obtain tailored release profiles for two drugs by tuning the filament composition and the design of the modular units. We have demonstrated that LEGO® -like designs can be introduced for the development of personalised dosage forms in the form of regular tablets for the treatment of sleeping disorders but also several other diseases that require dose adjustments and customised drug release rates to meet patients specific needs.

Declaration of Competing Interest

The authors declare that they have no known competing financial interests or personal relationships that could have appeared to influence the work reported in this paper.

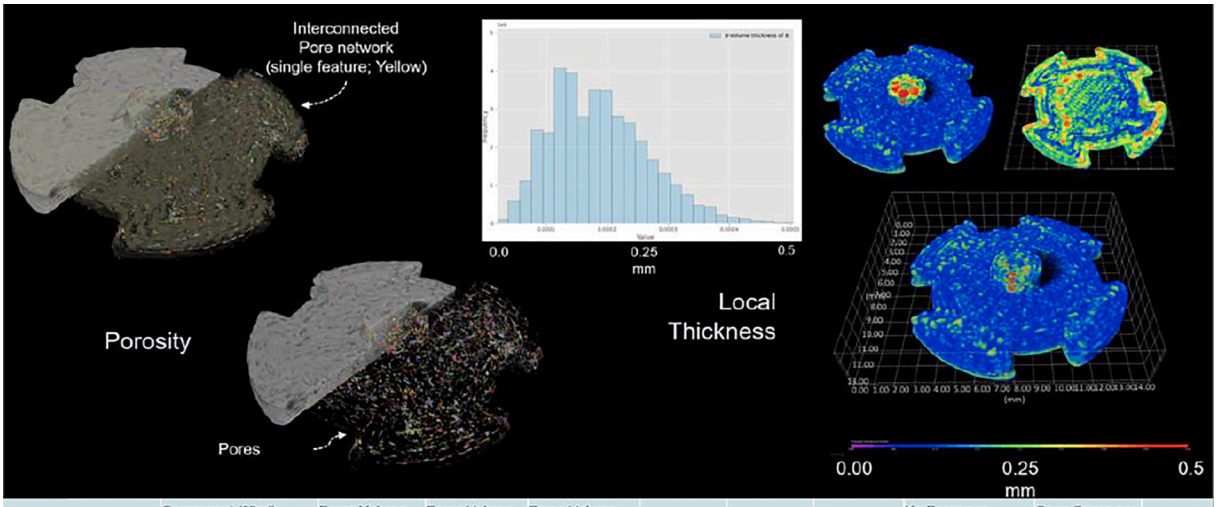

Component Volume ex. Open space (mm³)	Component (filled) volume incl OpenSpce (mm³)	Pores Volume incl OpenSpace Mean (mm³)	Pores Volume incl OpenSpace STD (mm²)	Pores Volume incl OpenSpace Median (mm³)	Pores Mean (mm³)	Pores STD (mm³)	Pores Median (mm³)	No Pores per Volume exOpenSpace	Open Space per Closed volume %	Porosity %
N/A	123.38	N/A	N/A	N/A	2.58E-03	2.31E-01	6.58E-05	77.96	N/A	20.2%

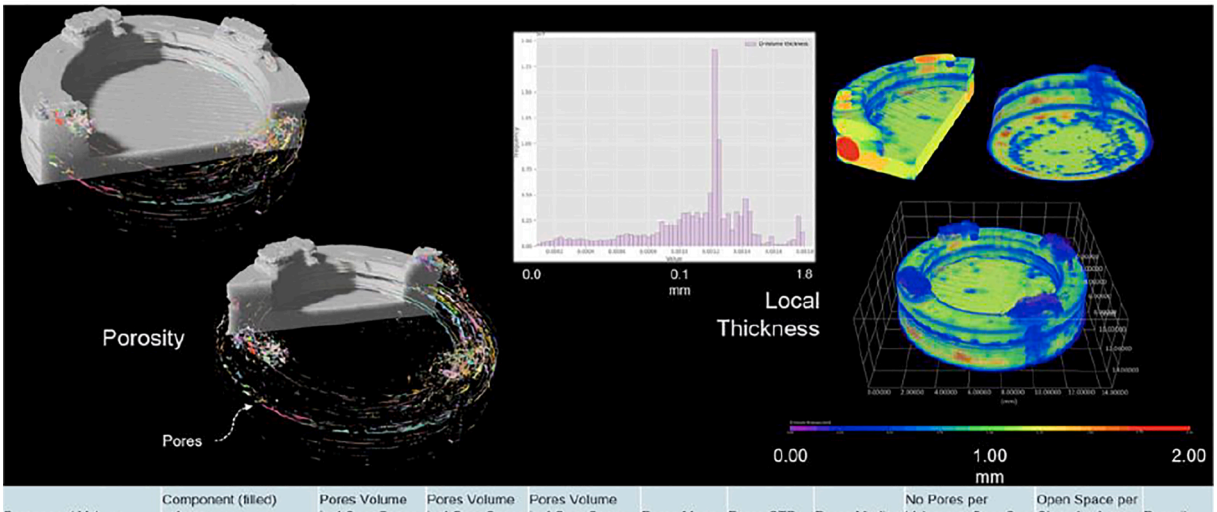

Component Volume ex. Open space (mm³)	Component (filled) volume incl OpenSpce (mm³)	Pores Volume incl OpenSpace Mean (mm³)	Pores Volume incl OpenSpace STD (mm²)	Pores Volume incl OpenSpace Median (mm³)	Pores Mean (mm³)	Pores STD (mm³)	Pores Median (mm³)	No Pores per Volume exOpenSpace	Open Space per Closed volume %	Porosity %
N/A	316.70	N/A	N/A	N/A	4.36E-04	1.74E-03	7.68E-05	7.62	N/A	0.3%

Fig. 8. a-b: Placebo compartments: Defects micro-porosity visualisation (left pane) and quantification (table). Both compartments were designed with 100% infill, so designed Open Space porosity is N/A. Thickness analysis (middle and left panes) showing the local thickness frequency of the compartments expressed as the diameter of the maximum fitting sphere containing each voxel.

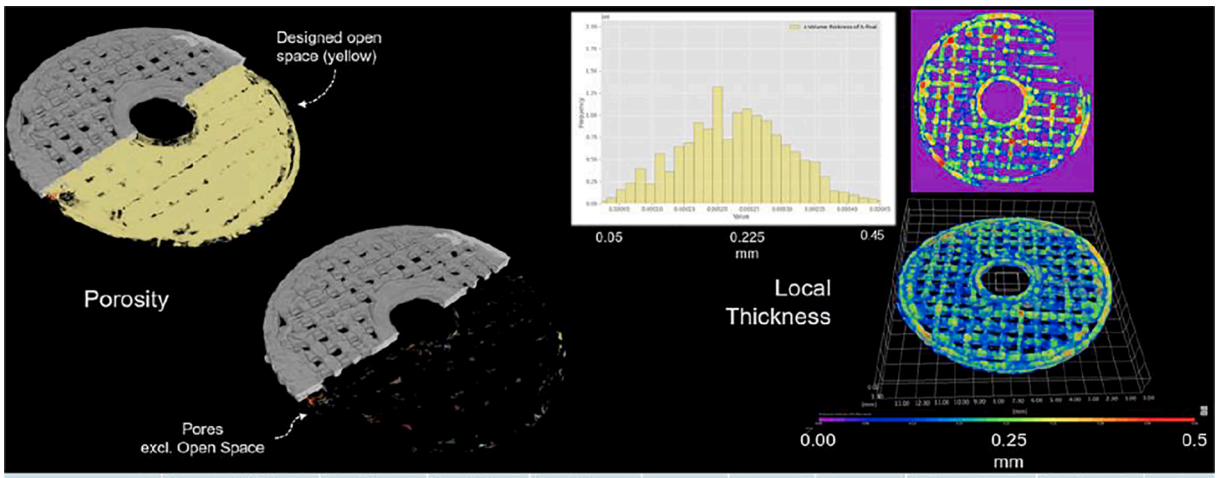

Component Volume ex. Open space (mm³)	Component (filled) volume incl OpenSpce (mm³)	Pores Volume incl OpenSpace Mean (mm³)	Pores Volume incl OpenSpace STD (mm³)	Pores Volume incl OpenSpace Median (mm³)	Pores Mean (mm³)	Pores STD (mm³)	Pores Median (mm³)	No Pores per Volume exOpenSpace	Open Space per Closed volume %	Porosity %
43.16	74.23	0.06	1.35	5.21E-05	1.98E-04	5.94E-04	5.21E-05	12.16	41.9%	0.2%

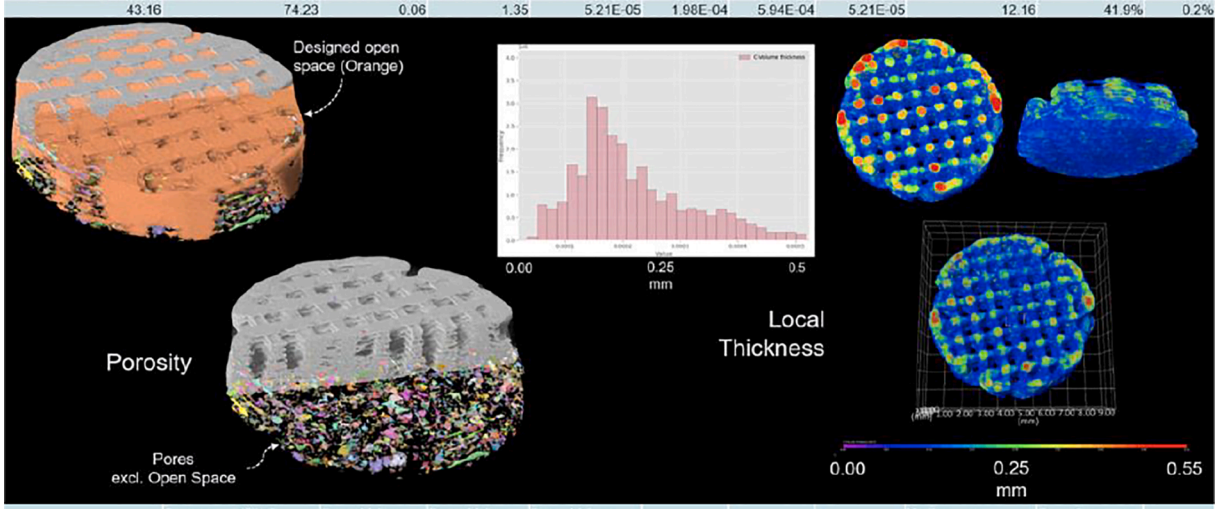

Component Volume ex. Open space (mm³)	Component (filled) volume incl OpenSpce (mm³)	Pores Volume incl OpenSpace Mean (mm³)	Pores Volume incl OpenSpace STD (mm³)	Pores Volume incl OpenSpace Median (mm³)	Pores Mean (mm³)	Pores STD (mm³)	Pores Median (mm³)	No Pores per Volume exOpenSpace	Open Space per Closed volume %	Porosity %
76.52	114.62	0.01	0.52	9.87E-05	3.15E-04	7.91E-04	9.87E-05	70.58	33.2%	2.2%

Fig. 9. c-d: CAF and MLT compartments: Open space - designed porosity (left-top pane) and defects porosity (left-bottom pane). Thickness analysis (middle and left panes) showing the local thickness distribution of the compartments expressed as the diameter of the maximum fitting sphere containing each voxel.

Data availability

Data will be made available on request.

Acknowledgements

Beamtime allocation at the μ-VIS X-ray Imaging Centre (www.muvis.org) was supported by the National Research Facility for Lab-based X-ray CT (nxct.ac.uk) through EPSRC grant EP/T02593X/1. The graphical abstract has been created using BioRender.com.

Appendix A. Supplementary material

Supplementary data to this article can be found online at https://doi.org/10.1016/j.ijpharm.2022.122574.

References

Araújo, M.R.P., Sa-Barreto, L.L., Gratieri, T., Gelfuso, G.M., Cunha-Filho, M., 2019. The digital pharmacies era: How 3D printing technology using fused deposition modeling can become a reality. Pharmaceutics.

Arendt, J., 1997. Safety of Melatonin in Long-Term Use(?). J. Biol. Rhythms. https://doi.org/10.1177/074873049701200624.

Bhaskar, S., Hemavathy, D., Prasad, S., 2016. Prevalence of chronic insomnia in adult patients and its correlation with medical comorbidities. J. Fam. Med. Prim. care 5, 780–784. https://doi.org/10.4103/2249-4863.201153.

Chao, M., Öblom, H., Cornett, C., Bøtker, J., Rantanen, J., Sporrong, S.K., Genina, N., 2021. Data-Enriched Edible Pharmaceuticals (DEEP) with Bespoke Design, Dose and Drug Release. Pharm. 13.

Christian, P., Ehmann, H.M.A., Coclite, A.M., Werzer, O., 2016. Polymer Encapsulation of an Amorphous Pharmaceutical by initiated Chemical Vapor Deposition for Enhanced Stability. ACS Appl. Mater. Interfaces 8, 21177–21184. https://doi.org/10.1021/acsami.6b06015.

Cunha-Filho, M., Araújo, M.R., Gelfuso, G.M., Gratieri, T., 2017. FDM 3D printing of modified drug-delivery systems using hot melt extrusion: A new approach for individualized therapy. Ther. Deliv. https://doi.org/10.4155/tde-2017-0067.

Dong, J.X., Li, Q., Tan, Z.C., Zhang, Z.H., Liu, Y., 2007. The standard molar enthalpy of formation, molar heat capacities, and thermal stability of anhydrous caffeine. J. Chem. Thermodyn. https://doi.org/10.1016/j.jct.2006.05.009.

Farzadi, A., Solati-Hashjin, M., Asadi-Eydivand, M., Osman, N.A.A., 2014. Effect of layer thickness and printing orientation on mechanical properties and dimensional accuracy of 3D printed porous samples for bone tissue engineering. PLoS One. https://doi.org/10.1371/journal.pone.0108252.

Ghanizadeh Tabriz, A., Nandi, U., Hurt, A.P., Hui, H.-W., Karki, S., Gong, Y., Kumar, S., Douroumis, D., 2020. 3D Printed Bilayer Tablet with Dual Controlled Drug Release for Tuberculosis Treatment. Int. J. Pharm. 120147 https://doi.org/10.1016/j.ijpharm.2020.120147.

Goyanes, A., Det-Amornrat, U., Wang, J., Basit, A.W., Gaisford, S., 2016. 3D scanning and 3D printing as innovative technologies for fabricating personalized topical drug delivery systems. J. Control. Release 234, 41–48. https://doi.org/10.1016/j.jconrel.2016.05.034.

Khaled, S.A., Alexander, M.R., Wildman, R.D., Wallace, M.J., Sharpe, S., Yoo, J., Roberts, C.J., 2018. 3D extrusion printing of high drug loading immediate release paracetamol tablets. Int. J. Pharm. 538, 223–230. https://doi.org/10.1016/j.ijpharm.2018.01.024.

Krause, J., Müller, L., Sarwinska, D., Seidlitz, A., Sznitowska, M., Weitschies, W., 2021. 3D Printing of Mini Tablets for Pediatric Use. Pharm. 14.

Kulinowski, P., Malczewski, P., Pesta, E., Łaszcz, M., Mendyk, A., Polak, S., Dorożyński, P., 2021. Selective laser sintering (SLS) technique for pharmaceutical applications—Development of high dose controlled release printlets. Addit. Manuf. 38, 101761 https://doi.org/10.1016/j.addma.2020.101761.

Lion, A., Wildman, R.D., Alexander, M.R., Roberts, C.J., 2021. Customisable Tablet Printing: The Development of Multimaterial Hot Melt Inkjet 3D Printing to Produce Complex and Personalised Dosage Forms. Pharm. 13.

Maroni, A., Melocchi, A., Parietti, F., Foppoli, A., Zema, L., Gazzaniga, A., 2017. 3D printed multi-compartment capsular devices for two-pulse oral drug delivery. J. Control. Release. https://doi.org/10.1016/j.jconrel.2017.10.008.

Martinez, P.R., Goyanes, A., Basit, A.W., Gaisford, S., 2018. Influence of Geometry on the Drug Release Profiles of Stereolithographic (SLA) 3D-Printed Tablets. AAPS PharmSciTech 19, 3355–3361. https://doi.org/10.1208/s12249-018-1075-3.

Melocchi, A., Uboldi, M., Parietti, F., Cerea, M., Foppoli, A., Palugan, L., Gazzaniga, A., Maroni, A., Zema, L., 2020. Lego-Inspired Capsular Devices for the Development of Personalized Dietary Supplements: Proof of Concept With Multimodal Release of Caffeine. J. Pharm. Sci. https://doi.org/10.1016/j.xphs.2020.02.013.

Pinho, L.A.G., Lima, A.L., Sa-Barreto, L.L., Gratieri, T., Gelfuso, G.M., Marreto, R.N., Cunha-Filho, M., 2021. Preformulation Studies to Guide the Production of Medicines by Fused Deposition Modeling 3D Printing. AAPS PharmSciTech. https://doi.org/10.1208/s12249-021-02114-7.

Ponsar, H., Wiedey, R., Quodbach, J., 2020. Hot-melt extrusion process fluctuations and their impact on critical quality attributes of filaments and 3d-printed dosage forms. Pharmaceutics. https://doi.org/10.3390/pharmaceutics12060511.

Rycerz, K., Stepien, K.A., Czapiewska, M., Arafat, B.T., Habashy, R., Isreb, A., Peak, M., Alhnan, M.A., 2019. Embedded 3D printing of novel bespoke soft dosage form concept for pediatrics. Pharmaceutics. https://doi.org/10.3390/pharmaceutics11120630.

Sadia, M., Isreb, A., Abbadi, I., Isreb, M., Aziz, D., Selo, A., Timmins, P., Alhnan, M.A., 2018. From 'fixed dose combinations' to 'a dynamic dose combiner': 3D printed bi-layer antihypertensive tablets. Eur. J. Pharm. Sci. 123, 484–494. https://doi.org/10.1016/j.ejps.2018.07.045.

Sandler, N., Preis, M., 2016. Printed Drug-Delivery Systems for Improved Patient Treatment. Trends Pharmacol. Sci. 37, 1070–1080. https://doi.org/10.1016/j.tips.2016.10.002.

Schindelin, J., Rueden, C.T., Hiner, M.C., Eliceiri, K.W., 2015. The ImageJ ecosystem: An open platform for biomedical image analysis. Mol. Reprod. Dev.

Scoutaris, N., Ross, S.A., Douroumis, D., 2018. 3D Printed "Starmix" Drug Loaded Dosage Forms for Paediatric Applications. Pharm. Res. 35, 34. https://doi.org/10.1007/s11095-017-2284-2.

Tabriz, A.G., Fullbrook, D.H., Vilain, L., Derrar, Y., Nandi, U., Grau, C., Morales, A., Hooper, G., Hiezl, Z., Douroumis, D., 2021. Personalised Tasted Masked Chewable 3D Printed Fruit-Chews for Paediatric Patients. Pharm. 13.

Tabriz, A.G., Scoutaris, N., Gong, Y., Hui, H.-W., Kumar, S., Douroumis, D., 2021. Investigation on hot melt extrusion and prediction on 3D printability of pharmaceutical grade polymers. Int. J. Pharm. 604, 120755 https://doi.org/10.1016/j.ijpharm.2021.120755.

Tagami, T., Ito, E., Kida, R., Hirose, K., Noda, T., Ozeki, T., 2021. 3D printing of gummy drug formulations composed of gelatin and an HPMC-based hydrogel for pediatric use. Int. J. Pharm. 594, 120118 https://doi.org/10.1016/j.ijpharm.2020.120118.

Tan, Y.J.N., Yong, W.P., Kochhar, J.S., Khanolkar, J., Yao, X., Sun, Y., Ao, C.K., Soh, S., 2020. On-demand fully customizable drug tablets via 3D printing technology for personalized medicine. J. Control. Release. https://doi.org/10.1016/j.jconrel.2020.02.046.

Wang, J., Goyanes, A., Gaisford, S., Basit, A.W., 2016. Stereolithographic (SLA) 3D printing of oral modified-release dosage forms. Int. J. Pharm. 503, 207–212. https://doi.org/10.1016/j.ijpharm.2016.03.016.

Xu, X., Robles-Martinez, P., Madla, C.M., Joubert, F., Goyanes, A., Basit, A.W., Gaisford, S., 2020. Stereolithography (SLA) 3D printing of an antihypertensive polyprintlet: Case study of an unexpected photopolymer-drug reaction. Addit. Manuf. 33, 101071 https://doi.org/10.1016/j.addma.2020.101071.